

## Bond of Hooked Glass Fiber Reinforced Plastic (GFRP) Reinforcing Bars to Concrete



by M. R. Ehsani, H. Saadatmanesh, and S. Tao

*The objective of this study was to determine the bond behavior of hooked glass fiber reinforced plastic (GFRP) reinforcing bars to concrete. Thirty-six 90 deg hooked reinforcing bar specimens were tested to examine the effects of concrete compressive strength, radius of bend, tail length, straight embedment length, and reinforcing bar diameter under monotonic static loading. The slip between the reinforcing bars and concrete was measured at the loaded end for various load levels. The tensile load was applied to the reinforcing bar until splitting of concrete or fracture of reinforcing bar occurred. The test results indicated that, with increases in concrete compressive strength, radius of bend, and straight embedment length, the ultimate tensile stress and initial stiffness increased and the maximum slip at failure decreased. The tail length beyond 12 bar diameters had little effect on the ultimate tensile stress. Based on a regression analysis of the test results, it is recommended that the development length of hooked GFRP bars be taken as 16 times the bar diameter.*

Keywords: bonding; fibers; glass; plastics; polymers and resins; reinforced concrete; reinforcing steels.

Ninety-deg hooks are commonly used in concrete construction for anchorage of tension reinforcement. The anchorage capacity of hooked reinforcing bars is provided by the bond along the straight embedment length, the hook itself, and the tail length.

Concrete reinforced with steel reinforcing bars has been used successfully in civil engineering for decades. However, the corrosion of these structures, particularly when they are located in such aggressive environments as coastal and marine structures, bridges, chemical plants, water and wastewater treatment facilities, etc., is of concern (Saadatmanesh and Ehsani 1991). Hundreds of millions of dollars are spent each year to repair corrosion-induced damage in concrete structures. Among methods adopted to prevent or delay the corrosion of steel reinforcing bars are inclusion of additives and admixtures to reduce the permeability of concrete and use of epoxy-coated steel reinforcing bars. The latter, when introduced in the early 1970s, was expected to be a major breakthrough in eliminating the corrosion of reinforcing bars. However, with the recent discovery of the extensive premature corrosion of epoxy-coated steel reinforcing bars in new construction (Keesler and Powers 1988), this hope has all but vanished. It is clear that no practical and economical ap-

proach currently exists to prevent corrosion of reinforcing bars. Efficient techniques or new materials are needed to solve this problem.

Recently, glass fiber reinforced plastic (GFRP) reinforcing bars have been introduced that promise to be more durable than steel reinforcing bars. GFRP reinforcing bars offer significant advantages over conventional reinforcing steel, such as resistance to corrosion, high strength, light weight, ease of handling on the job site, and ease of cutting. A major reason limiting use of GFRP reinforcing bars is lack of information on their bond behavior.

To determine the effect of bond length, bend angle, bend radius, and bar diameter on the deformation and strength of hooked steel bars, Minor and Jirsa (1975) examined 80 specimens containing bars bent to different geometric configurations. The test results indicated that, at a given bar stress, the larger the angle of bend or the smaller the radius of bend, the greater the slip. For practical joint design detailing, 90-deg hooks are preferable to 180-deg hooks and, to reduce slip, the radius of the hook should be as large as practical.

Bond stress-slip relationships of FRP reinforcing bars in concrete were studied by Larralde and Silva (1993). In pull-out testing, the concrete surrounding the reinforcing bars is under compression, reducing the possibility of cracking and increasing the bond strength due to Poisson's effect. In contrast, in concrete beams, the concrete surrounding the reinforcing bars is under tension, thus, allowing for cracking at lower stresses and reducing friction. Consequently, the nominal bond strength obtained from pullout tests does not reflect the actual conditions in flexural reinforced concrete members, and is greater than the nominal bond strength obtained from reinforcing bars under flexural tension. In addition, from the experimental results, it was concluded that the anchorage design for steel reinforcing bars is not directly applicable to FRP reinforcing bars. Under the same test condi-

*ACI Materials Journal*, V. 92, No. 4, July-August 1995.

Received Jan. 30, 1994, and reviewed under Institute publication policies. Copyright © 1995, American Concrete Institute. All rights reserved, including the making of copies unless permission is obtained from the copyright proprietors. Pertinent discussion will be published in the May-June 1996 *ACI Materials Journal* if received by Feb. 1, 1996.

ACI member **Mohammad R. Ehsani** is an associate professor of civil engineering and engineering mechanics at the University of Arizona. He is a member of ACI Committee 408, Bond and Development of Reinforcement, where he chairs a subcommittee on bond of FRP reinforcing bars. As a member of ACI Committee 440, Fiber Reinforced Plastic Reinforcement, he chairs a subcommittee on the state of the art report. He is also Secretary of joint ACI/ASCE Committee 352, Joints and Connections in Monolithic Concrete Structures. Dr. Ehsani is a registered professional engineer in Arizona and California.

**Hamid Saadatmanesh** is an associate professor of civil engineering and engineering mechanics at the University of Arizona. He is Secretary of ACI Committee 440, Fiber Reinforced Plastic Reinforcement. His areas of research interest include application of advanced composite materials for reinforcing and strengthening of concrete structures and nondestructive evaluation of materials. He is a registered professional engineer in California.

**S. Tao** is a doctoral candidate in civil engineering at the University of Arizona. He received his BS and MS degrees in civil engineering from Beijing Polytechnic University. His research interests include reinforced concrete structures and the application of advanced composite materials in civil engineering structures.

tions, the average nominal bond stress at failure was greater for the steel reinforcing bars than for the FRP reinforcing bars. The slips of the reinforcing bars relative to the concrete surface were greater for the FRP reinforcing bars than for steel reinforcing bars.

The principal objective of this research project was to determine the bond behavior of straight and hooked GFRP reinforcing bars to concrete. A total of 102 specimens were tested. Based on these data, analytical expressions have been presented for basic development length of straight and hooked GFRP reinforcing bars to concrete. Due to space limitation, however, this paper will discuss the study of bond behavior of hooked GFRP reinforcing bars to concrete only. The study on bond behavior of straight GFRP reinforcing bars to concrete, and the development of design guidelines for bond of GFRP reinforcing bars to concrete, are presented elsewhere (Tao 1994).

### RESEARCH SIGNIFICANCE

Few experimental data are available in the literature on bond behavior of hooked GFRP reinforcing bars to concrete. In addition, the guidelines provided in ACI 318-89 for bond of hooked steel reinforcing bars cannot be directly utilized for GFRP reinforcing bars due to the major differences that exist in tensile strength, modulus of elasticity, and deformation patterns of GFRP and steel reinforcing bars. The study reported herein provides information on the bond behavior of hooked GFRP reinforcing bars to concrete.

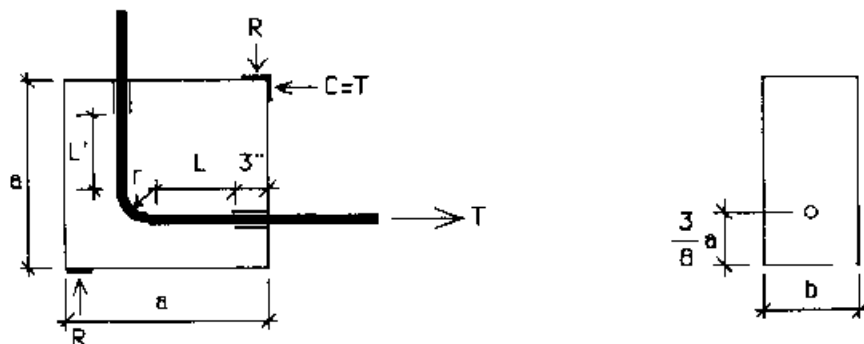


Fig. 1—Test specimens

Table 1—Dimensions of test specimens

Reinforcing bar size	a, in.	b, in.
No. 3	12	8
No. 6	18	10
No. 9	24	12

Note: 1 in. = 25.4 mm.

### EXPERIMENTAL PROGRAM

The main purpose of the research reported in this paper was to investigate the influence of several parameters on bond behavior of hooked GFRP reinforcing bars to concrete. Thirty-six specimens were constructed and tested under static monotonic loading. Variables in the specimens included concrete compressive strength, radius of bend, tail length, straight embedment length, and reinforcing bar diameter. The ultimate applied load, ultimate tensile stress, loaded-end slip, mode of failure, and load-slip relationship were obtained from these tests.

### Design of specimens

A sketch of a typical test specimen is shown in Fig. 1, and the corresponding dimensions are listed in Table 1.

Each specimen was cast in the position shown in Fig. 1, with the lead-in portion of the hook in a horizontal position at a distance of three-eighths of the height  $a$  from the bottom surface of the specimen. No transverse reinforcement was used within the specimens.

To eliminate the influence of the support reactions on the loaded end, the first 3 in. (76 mm) of the reinforcing bar was wrapped in a thin conduit to prevent its bonding to concrete (Fig. 1). Therefore, by careful placement of the reinforcing bar prior to casting, the desired straight embedment length  $L$ , i.e., the distance between the beginning of the bend and the point of 3 in. (76 mm) from the concrete face, was obtained for all specimens.

The tail length of standard hooked steel reinforcing bars is 12 bar diameters. To investigate the potential benefits of longer tail lengths, some specimens were cast with hooks with tail lengths  $L'$  20 times the bar diameter.

Because bending of steel reinforcing bars through small radii could result in the fracture of the bar, ACI 318-89 requires minimum radii of bend. In GFRP reinforcing bars, however, it is possible to bend the uncured reinforcing bar during the manufacturing process through smaller radii. For this study, the ratios of radius to reinforcing bar diameter

**Table 2—Reinforcing bar dimensions**

Property	No. 3	No. 6	No. 9
Rib height, in.	0.045	0.051	0.079
Pitch, in.	0.687	0.938	1.063
Angle, deg	37	25	23
Measured diameter, in.	0.381	0.726	1.079
Nominal diameter, in.	0.375	0.750	1.125
Measured diameter/nominal diameter	1.016	0.968	0.959

Note: 1 in. = 25.4 mm

**Table 3—Data for modulus of elasticity**

Reinforcing bar no.	Sample 1, ksi	Sample 2, ksi	Sample 3, ksi	Average for three samples, ksi
3	6750	6824	6857	6810
6	7028	7115	7001	7050
9	7281	7298	7257	7280

Note: 1 ksi = 6.895 MPa

**Table 4—Data for ultimate tensile strength**

Reinforcing bar no.	Sample 1, ksi	Sample 2, ksi	Sample 3, ksi	Average for three samples, ksi
3	129	141	135	135
6	98	93	88	93
9	77	76	78	77

Note: 1 ksi = 6.895 MPa

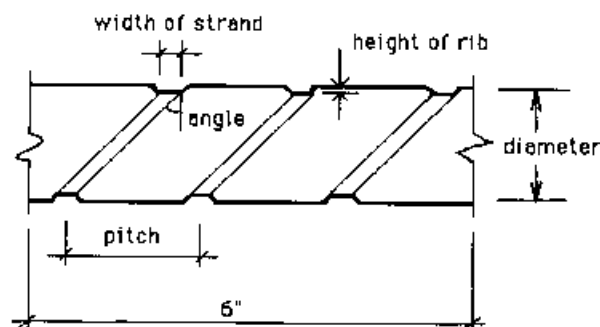


Fig. 2—Sample for measuring rib geometry

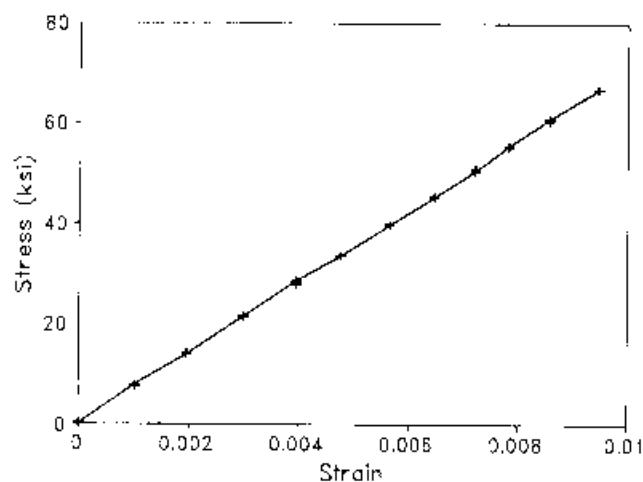


Fig. 3—Tension stress-strain relationship for GFRP reinforcing bars

were selected as zero and 3 to examine the effect of the radius of bend.

### Material properties

The concrete used in this study was obtained from a ready-mix plant and specified to have a nominal compressive strength of 4000 and 8000 psi (28 and 56 MPa). The concrete aggregate had a maximum size of 1 in. (25 mm). Sixteen standard 6 x 12-in. (152 x 305-mm) cylinders were cast at the same time and cured under the same condition as the specimens for each concrete batch.

The GFRP reinforcing bars used in the research program were supplied by a U.S. manufacturer in the nominal diameters of 0.375, 0.75, and 1.125 in. (10, 19, and 29 mm). These reinforcing bars were manufactured using the pultrusion process and were made of polyester resin and Type E glass fibers, with 72 percent glass and 38 percent resin by volume, respectively. Additional fiberglass strands were wrapped around the reinforcing bars in a helical pattern to enhance bond characteristics. The width of the strands wrapped around the outside diameter is usually the same for all manufactured sizes. As shown in Fig. 2, the pitch is defined as the distance from center-to-center of the helical strand. Larger diameter reinforcing bars had longer pitches.

The reinforcing bar diameters were measured by the volumetric method, cutting a representative 6-in. (152-mm) sample, submerging the sample in a graduated cylinder, and

measuring the change in volume. The cross-sectional area of the bar was calculated by dividing its volume by the 6-in. (152-mm) length. Assuming a circular cross section for the reinforcing bar, the average diameter was calculated. Diameter measurements taken at different sections resulted in slight differences between the measured and nominal diameters, which are listed in Table 2.

The ultimate tensile strength and stiffness were measured by subjecting GFRP bars to uniaxial tension tests. These bars had a gage length of approximately 20 in. (508 mm). A typical stress-strain curve is shown in Fig. 3. All tension tests of GFRP reinforcing bars showed a similar linear relationship for the entire loading range. Test results for modulus of elasticity and ultimate tensile strength of reinforcing bars are presented in Tables 3 and 4, respectively.

As seen in Table 3, the modulus of elasticity for GFRP reinforcing bars is almost constant and averages around 7000 ksi (48,270 MPa). But the results in Table 4 reveal that the ultimate tensile strength is sensitive to reinforcing bar diameters, and decreases rapidly with an increase in reinforcing bar diameter. Since the tensile load was applied along the GFRP reinforcing bar by friction mechanism between the sand-coated grips and reinforcing bar surface, loading was likely to induce a parabolic and axisymmetric strain distribution across the cross section of the reinforcing bar (Wu, Gangarao, and Prucz 1991). Thus, strength reduction with reinforcing bar diameter is due to the shear lag phenomenon.

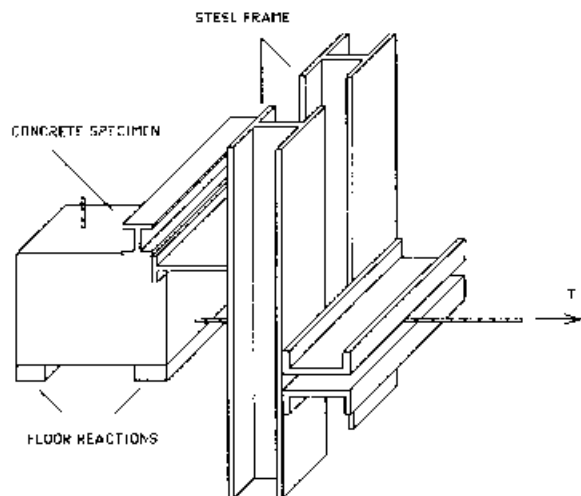


Fig. 4—Test setup for specimens

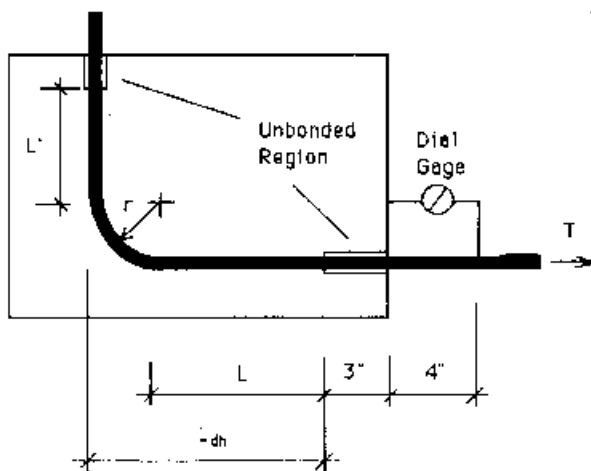


Fig. 5 Dial gage setup

### Test setup and instrumentation

The test setup for the specimens is shown in Fig. 4. Due to the low shear strength of the reinforcing bars, care must be taken not to harm the reinforcing bar during placement of the specimens in the test frame.

In earlier studies, the design and development of suitable grips to pull GFRP reinforcing bars embedded in concrete have presented some difficulties. Because glass fiber-based composites are very weak for loads applied transverse to the fiber directions, the region of the GFRP reinforcing bar in the grip must be protected against crushing (Ehsani, Saadatmanesh, and Tao 1993). The grip must grasp the reinforcing bar in such a manner as to avoid failure of the reinforcing bar at the grips, allowing the failure to take place away from the grip region (Paza and GangaRao 1990). A specially constructed set of sand-coated grips similar to those used in testing of GFRP reinforcing bars at West Virginia University was employed. The applied loads are transmitted from the jack to the GFRP reinforcing bars through these grips. The tests were successful in avoiding excessive slippage or reinforcing bar failure in the grip region. The sand-coated grips proved effective for all reinforcing bar sizes.

Monotonic static loading was gradually applied in approximately constant increments of 1000 lb (4.45 kN) until splitting failure of concrete or fracture of reinforcing bar was

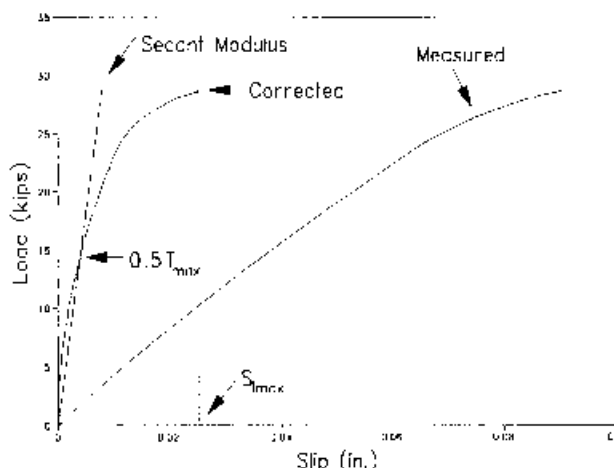


Fig. 6—Typical load-slip relationship

reached. The load values were measured by two load cells and automatically recorded by an automatic data acquisition control system. Meanwhile, slip was measured at each load level during testing by reading a 0.0001-in. dial gage attached at the loaded end of the reinforcing bar, as seen in Fig. 5.

### TEST RESULTS

Results of the 36 specimens were examined to evaluate the bond behavior of hooked GFRP reinforcing bars to concrete. Under monotonic static loading, the load values and loaded-end slips were obtained at each load increment. The corresponding nominal tensile stress was calculated as the applied tensile load divided by the nominal cross section of the reinforcing bar, or

$$f_s = \frac{4T}{\pi d_b^2} \quad (1)$$

where  $f_s$  = tensile stress,  $T$  = applied tensile force, and  $d_b$  = reinforcing bar diameter.

Fig. 6 shows a typical plot of the applied load versus the slip at the loaded end of the reinforcing bar. As seen in the curve, the loaded end started to slip from the beginning of the loading, and continued until splitting failure or reinforcing bar fracture occurred.

The measured loaded-end slip contains two main components: elastic elongation of the reinforcing bar itself, and slip of the reinforcing bar with respect to the surrounding concrete. Note that, due to the relatively high modulus of steel, the former component is usually ignored in bond studies of steel reinforcing bars. However, in the case of GFRP bars, the contribution of this component to the total measured displacement cannot be ignored.

As shown previously in Fig. 5, the dial gage attached to the loaded end of the reinforcing bar measured the movement of a point 4 in. (102 mm) away from the concrete block relative to the face of the block. In addition, the first 3 in. (76 mm) of the reinforcing bar was always shielded to prevent its bonding to concrete. Therefore, the measured slip at the loaded end of the reinforcing bar included the elastic elongation of the 7-in. (178-mm) lead length. Due to the low modulus of

**Table 5—Test results**

Specimen	$f'_c$ , psi	$T_m^*$ , kips	$T_m^*/T_u$	$f_s^*$ , ksi	$S_{m,max}$ , in.	$E_p$ , k/in.	Failure mode
43H3124	5080	6.10	0.55	56	0.2234	88	S
43H3204	5080	5.80	0.53	53	0.2231	96	S
43H3127	4280	7.50	0.68	68	0.1453	268	S
43H31210	4280	8.80	0.79	80	0.1342	414	S
43H31213	4280	10.5	0.94	95	0.0388	523	RA
43H31216	4280	11.4	1.03	103	0.0282	776	RA
83H3124	6640	7.00	0.63	63	0.1672	128	S
83H3204	6640	6.90	0.62	62	0.1786	129	S
43H0121	5080	2.40	0.21	21	0.3114	43	RS
43H0201	5080	2.40	0.21	21	0.3165	43	RS
83H0121	6640	2.30	0.21	21	0.3044	45	RS
83H0201	6640	2.40	0.22	22	0.3089	46	RS
46H3124	5680	20.2	0.68	46	0.1786	604	S
46H3204	5680	20.6	0.70	47	0.1678	620	S
46H3127	4280	24.0	0.81	54	0.1111	1111	S
46H31210	4280	25.4	0.86	58	0.0989	2192	S
46H31213	4280	28.7	0.97	65	0.0256	3629	RA
46H31216	4280	29.4	1.00	67	0.0155	4592	RA
86H3124	6920	22.1	0.75	50	0.1231	788	S
86H3204	6920	22.3	0.76	50	0.0988	748	S
46H0121	5680	6.90	0.23	16	0.2514	110	RS
46H0201	5680	6.60	0.23	15	0.2487	109	RS
86H0121	6920	6.50	0.22	15	0.2322	115	RS
86H0201	6920	6.50	0.22	15	0.2291	116	RS
49H3124	5760	31.9	0.61	32	0.1111	1525	S
49H3204	5760	32.2	0.62	32	0.1231	1548	S
49H3127	4280	37.9	0.73	38	0.0897	3508	S
49H31210	4280	41.4	0.79	42	0.0655	4704	S
49H31213	4280	49.1	0.94	49	0.0161	8467	RA
49H31216	4280	51.6	0.99	52	0.0152	9554	RA
89H3124	6860	34.3	0.66	35	0.0876	2174	S
89H3204	6860	35.0	0.67	35	0.0879	2082	S
49H0121	5760	14.2	0.27	14	0.2148	177	RS
49H0201	5760	14.2	0.27	14	0.2177	177	RS
89H0121	6860	14.1	0.27	14	0.2054	185	RS
89H0201	6860	14.0	0.27	14	0.2089	184	RS

elasticity of GFRPs, this elongation is significant and has to be corrected. Thus, the actual slip was calculated as the difference between the measured slip at the loaded end and the elastic deformation, or

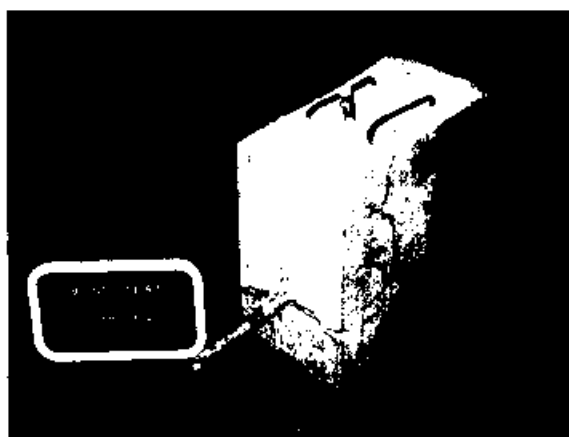
$$\delta_{s'} = \delta_m - \delta_e \quad (2)$$

Test results for all specimens are presented in Table 5. Notation for the specimens is as follows: the first number indicates the design concrete compressive strength in ksi; the second number is the reinforcing bar diameter; the letter "H" denotes a hooked reinforcing bar specimen; the third number is the ratio of radius to reinforcing bar diameter; the next number is the ratio of tail length to reinforcing bar diameter; and the last number is the ratio of the development length to reinforcing bar diameter. For example, 43H3124 designates a hooked specimen cast with 4000-psi (28-MPa) concrete, No. 3 GFRP reinforcing bar, where the ratios of radius, tail

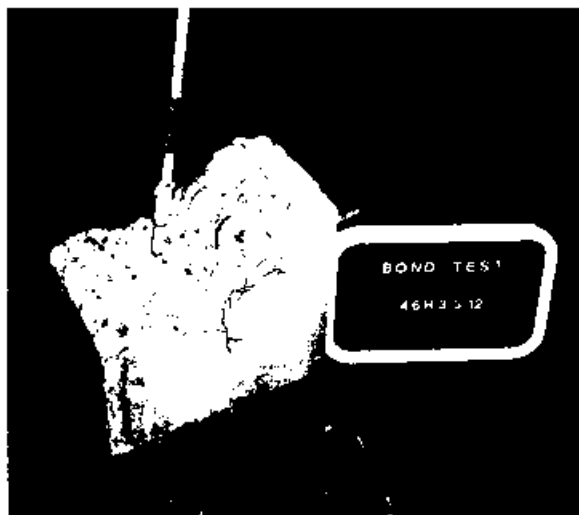
length, and development length to reinforcing bar diameter were 3, 12, and 4, respectively.

Due to variations in the concrete strength of specimens, it was necessary to normalize the test results with respect to an average concrete compressive strength to allow a reasonable comparison among specimens. The process for determining the average compressive strength was as follows. Specimens 46H3127, 46H31210, 46H31213, and 46H31216, for example, tested at approximately the same time, and three 6 x 12-in. (152 x 305-mm) cylinder tests resulted in an average compressive strength  $f'_c$  of 4280 psi (29.5 MPa), tabulated in the second column of Table 5. Next, an average concrete compressive strength  $f'_{c,avg}$  was calculated for all specimens expected to have a nominal concrete strength of 4000 or 8000 psi (28 or 56 MPa). These averages were 4890 and 6810 psi (34 and 47 MPa), respectively.

Earlier studies have indicated that bond strength varies with the square root of the compressive strength (Ferguson and Thompson 1962). To compare the test results directly, effects of the slight variations in the concrete compressive



(a)



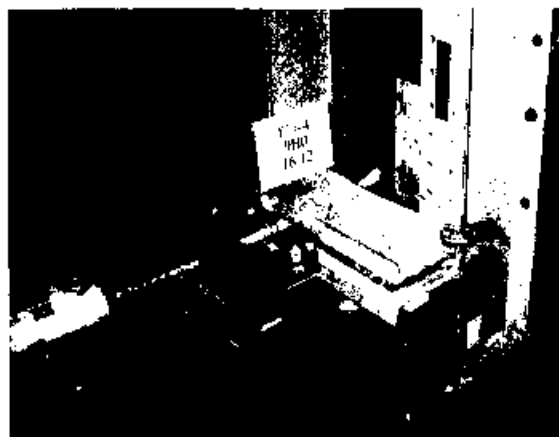
(b)

Fig. 7 (a) and (b)—Typical cracking pattern and failure of specimens due to splitting of concrete

strength had to be eliminated. Since the bond strength is proportional to the square root of the concrete strength, the maximum applied load values  $T_m$  and the corresponding tensile stress  $f_s$  have been multiplied by the factor  $\sqrt{f_{avg}'/f_c'}$  and listed as  $T_m^*$  and  $f_s^*$  in Columns 3 and 5, respectively, of Table 5.

The ratio  $T_m^*/T_u$  is listed in the fourth column of Table 5. The values of  $T_m^*$  are the maximum load applied along the reinforcing bar during the test. The values of  $T_u$  represent the ultimate tensile force of a reinforcing bar sample, calculated as the product of the average ultimate tensile strength reported in Table 4, multiplied by the minimum area for each reinforcing bar, calculated from the minimum bar diameter reported in Table 2. While this ratio is expected to be less than or equal to 1, it is occasionally slightly larger. This happens when the reinforcing bar fractures outside the specimen and tensile strength of reinforcing bar is slightly higher than its average ultimate tensile strength reported in Table 4.

During testing, the slip at the loaded end is expected to increase with an increase in loading. As shown in Fig. 6, the maximum slips listed in Column 6 of Table 5 correspond to those measured under maximum applied load and after the



(a)



(b)

Fig. 8—Typical failure of specimens due to fracture of reinforcing bars: (a) fracture of reinforcing bar near bend for specimens with  $\lambda/d_b = 0$ ; (b) fracture of reinforcing bar outside concrete for specimens with  $\lambda/d_b = 3$

necessary reduction for the elastic elongation of the lead length.

One way to compare the performance of different specimens is in terms of their stiffness. Because the service load stresses in GFRP reinforcing bars are expected to remain well below 50 percent of their ultimate strength, the initial stiffness  $E_f$  was defined as a secant modulus passing through the point of  $0.5 T_{max}$  (Fig. 6). These values are also given in Table 5.

Failure of hooked reinforcing bar specimens occurred either by splitting failure of concrete (S) or by fracture of reinforcing bar (RA-axial, RS-shear). The failure mode for each specimen is also listed in Table 5.

In nearly all splitting failures, such as that shown in Fig. 7, the cracking patterns were quite similar. During testing, horizontal cracks radiated outward from the reinforcing bar on the front face and propagated to side faces of the specimens. The vertical cracks appeared on the side faces and continued to the top face of the specimens with subsequent loading. The cracks were widened, and more cracks occurred with additional loading. Concrete splitting failure was sudden and ended with the side cover spalling away and reduction in the load. After removing the spalled side cover from a few spec-

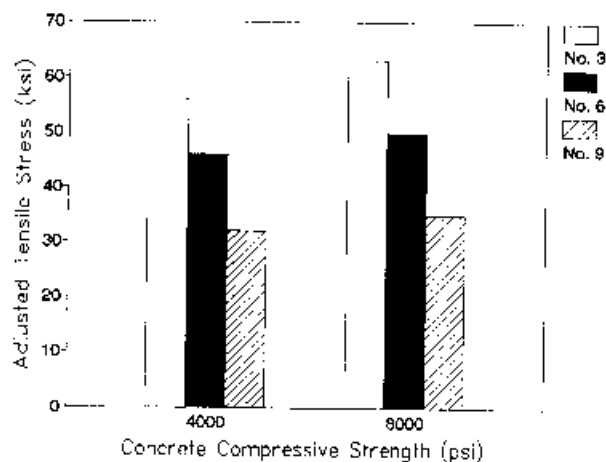


Fig. 9—Influence of concrete compressive strength on tensile stress for bars with  $r/d_b = 3$

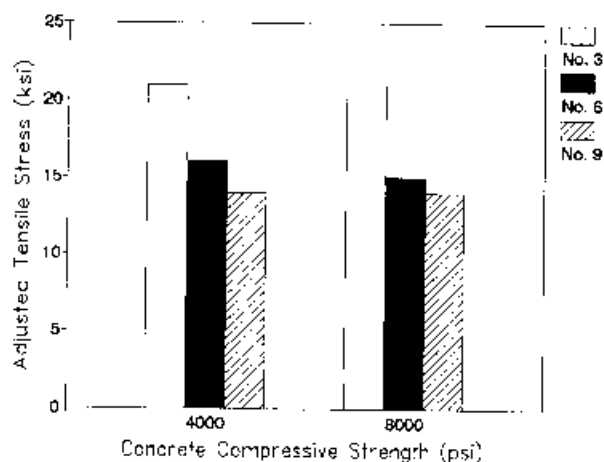


Fig. 10—Influence of concrete compressive strength on tensile stress for bars with  $r/d_b = 0$

imens, close examination at bend region of the bars indicated that the concrete at the inner radius of the bend was crushed completely. This behavior was induced by a wedge mechanism that produced intense compressive stresses to the concrete at the hook location.

As seen in Fig. 8, for specimens with  $r/d_b$  of zero, the reinforcing bars failed in shear at the hook under very low load levels. For specimens with  $r/d_b$  of 3, however, two modes of failure were observed. When the cover concrete or the straight embedment length was small, the specimens failed by splitting of concrete. Otherwise, the mode of failure was due to fracture of the reinforcing bar outside of the specimen.

## INFLUENCE OF DESIGN PARAMETERS

### Effect of concrete compressive strength

The anchorage capacity of hooked reinforcing bars is provided by the bond along the straight embedment length, the hook itself, and the tail length. Bond failure could be caused by tensile splitting of the concrete along the straight portion of the bar. Thus, the tensile strength of concrete, which is approximately proportional to the square root of its compressive strength, is considered a key parameter in bond behavior (ACI Committee 408, 1992). To determine the effect of concrete strength on the bond behavior of hooked GFRP reinforcing bars, compressive strengths of 4000 and 8000 psi (28 and 56 MPa) were selected for this study.

For specimens with  $r/d_b$  of 3, Fig. 9 illustrates the influence of concrete compressive strength on bond properties. The six specimens shown in this figure, 43H3124 and 83H3124, 46H3124 and 86H3124, and 49H3124 and 89H3124, had the same design parameters except for concrete compressive strength. It can be seen that the tensile stress of the reinforcing bar increases slightly with an increase in concrete strength. As shown in Fig. 10, however, concrete compressive strength has little influence on tensile stress for specimens with  $r/d_b$  of zero.

Comparison of Specimens 46H3124 and 86H3124 presented in Fig. 11 indicates that higher concrete compressive strength results in greater initial stiffness and smaller slip. The influence of concrete compressive strength on tensile stress of reinforcing bars, initial stiffness, and loaded-end

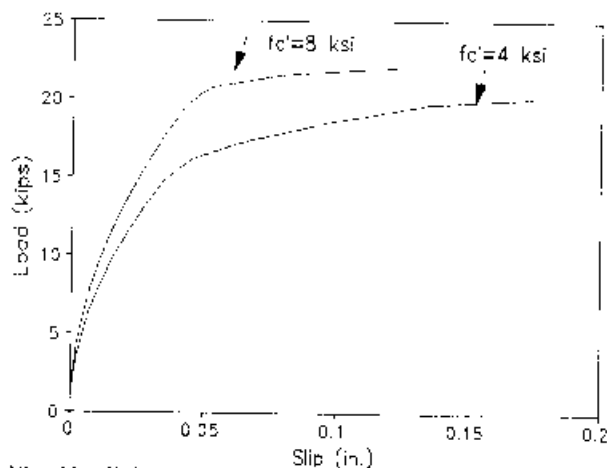


Fig. 11—Effect of concrete compressive strength on initial stiffness and slip

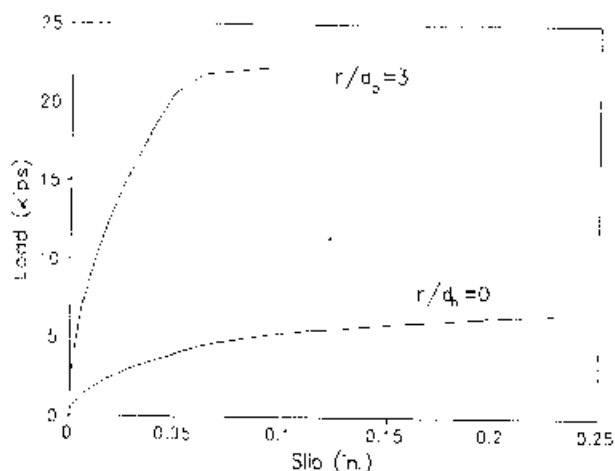


Fig. 12—Influence of hook radius on load-slip relation

slip was found to be similar for all other specimens with identical hook configurations.

### Effect of hook radius

For steel reinforcing bars, limits have been set for the radius of curvature of the hook to prevent fracture of the reinforcing bar. For GFRP reinforcing bars, however, this

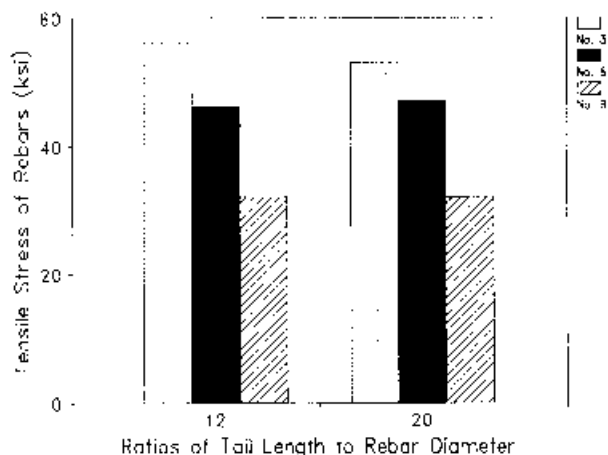


Fig. 13—Effect of tail length on tensile stress of reinforcing bars

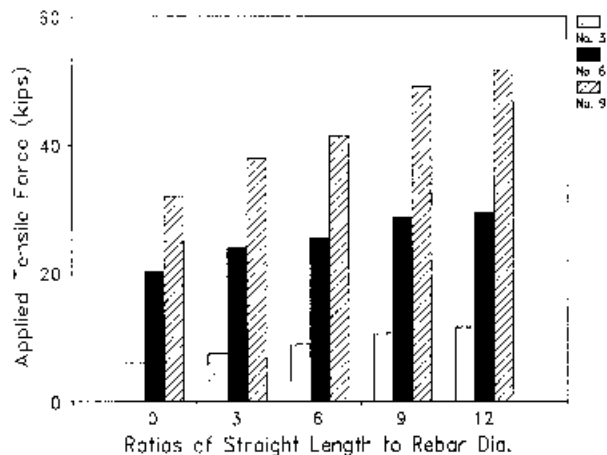


Fig. 16—Effect of straight embedment length on tensile force

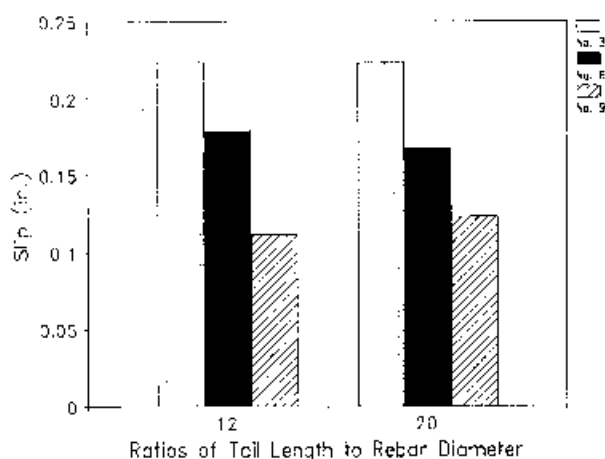


Fig. 14—Effect of tail length on loaded-end slip

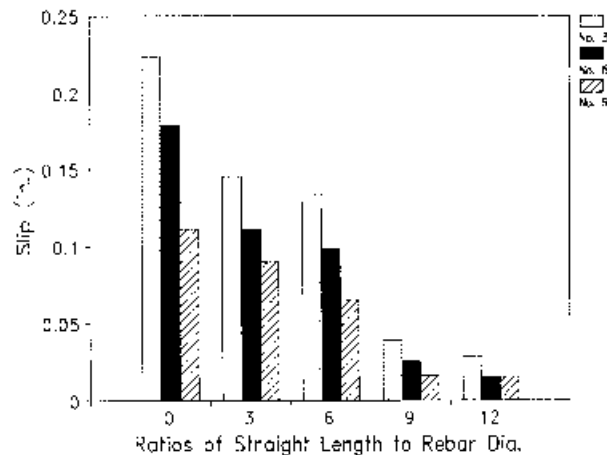


Fig. 17—Effect of straight embedment length on slip

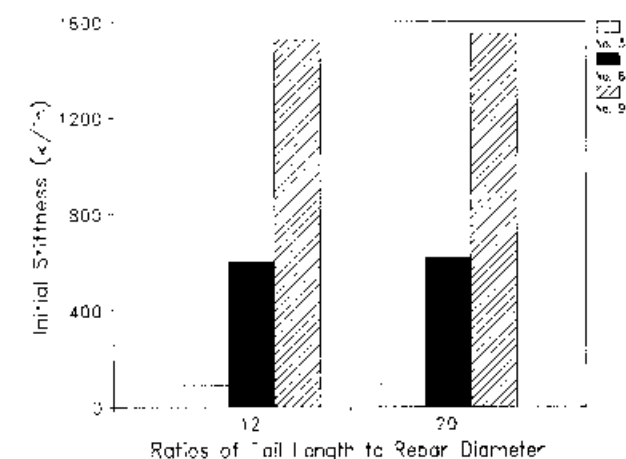


Fig. 15—Effect of tail length on initial stiffness

limitation does not apply because the bars are formed into their final shape before the resin is cured (Ehsani 1993). Two ratios of radius to reinforcing bar diameter, 3 and zero, were chosen to study the effect of hook radius on bond behavior. Fig. 12 shows the load-slip relation for Specimens 86H0201 and 86H3204. In this case, all hook geometry conditions except for hook radius are the same. As indicated, both the load and initial stiffness increased with an increase in the hook ra-

dius. In addition, for specimens with  $r/d_b$  of zero, the reinforcing bars failed in shear at very low load levels at the point when the horizontal and vertical legs of the bar intersected. Therefore, although manufacturing of GFRP reinforcing bars with sharp bends does not pose any difficulties, use of such details should be avoided due to the low shear strength of GFRPs. Additional studies are needed to determine the economy of using larger hook radii for GFRP bars and their effect on reducing the required development length.

#### Effect of tail length

The tensile force applied to the reinforcing bar was transferred to the concrete along the straight embedment length, the hook, and the partial tail length near the hook bend. Fig. 13 through 15 compare the data for Specimens 43H3124 and 43H3204, 46H3124 and 46H3204, and 49H3124 and 49H3204. As can be seen, a tail length of 20 times the bar diameter had no beneficial effect on the tensile stress of the reinforcing bars, the loaded-end slip, and the initial stiffness, compared to that of a standard hook with a tail length of 12 bar diameters. Therefore, longer tail lengths beyond  $12d_b$  had no significant influence on tensile stress and loaded-end slip. Moreover, initial stiffness is independent of longer tail

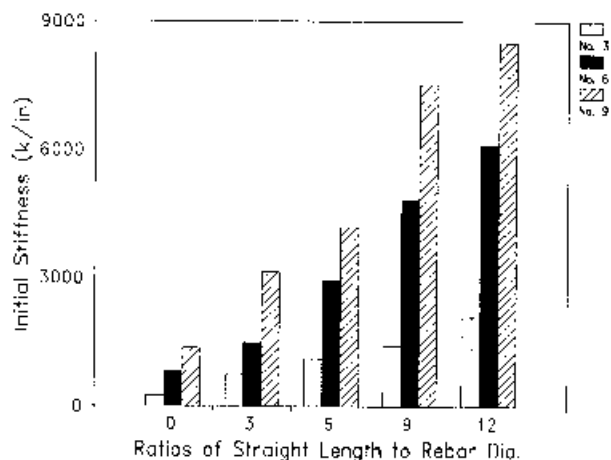


Fig. 18—Effect of straight embedment length on initial stiffness

lengths. The tail length of 12 bar diameters is long enough to sustain the applied tensile force during testing for all No. 3, 6, and 9 reinforcing bar specimens. Therefore, hooked GFRP reinforcing bars manufactured with tail lengths of 12 times the bar diameter are recommended for use in design.

#### Effect of straight embedment length

The straight embedment length refers to that portion of the bar between the beginning of the bend and the point 3 in. (76 mm) away from the concrete surface (Fig. 5). As shown in Fig. 16 through 18, straight embedment length has a significant influence on the applied tensile load, loaded-end slip, and initial stiffness. The specimens considered were cast with 4000-psi (28-MPa) concrete. The hooked GFRP reinforcing bars were selected with  $r/d_b$  of 3 and tail lengths of 12 times the bar diameter. As expected, the applied tensile load and initial stiffness increased with an increase in the straight embedment length. The loaded-end slip, however, decreased with an increase in the straight embedment length.

#### DESIGN RECOMMENDATIONS

Overall, behavior of the 36 specimens was examined to develop some preliminary design guidelines. To determine conservative conclusions, only the response of the specimens with lower strength concrete (i.e., 4000 psi) was considered. Additionally, because behavior of the specimens with  $r/d_b = 0$  was unsatisfactory, these were excluded from any further considerations. Similarly, small gains resulting from longer tail lengths were ignored. This resulted in a subset of specimens with designation 4\*H312\*, where "\*" can assume any of the previously described values.

For all specimens in the subset, ratios of the applied tensile force to the ultimate tensile capacity of the reinforcing bar ( $T_m/T_u$ ) for various straight embedment lengths have been plotted in Fig. 19. A ratio of at least 1.0 would indicate satisfactory bond performance, since the failure would be caused by the fracture of the reinforcing bar at a point away from the hook. As shown in Fig. 19, an increase in the straight embedment length improves this ratio. The bond capacity of the hook itself, i.e., when  $l/d_b = 0$ , is not sufficient to develop the tensile capacity of the hook. A regression analysis was performed to obtain the best-fit line passing

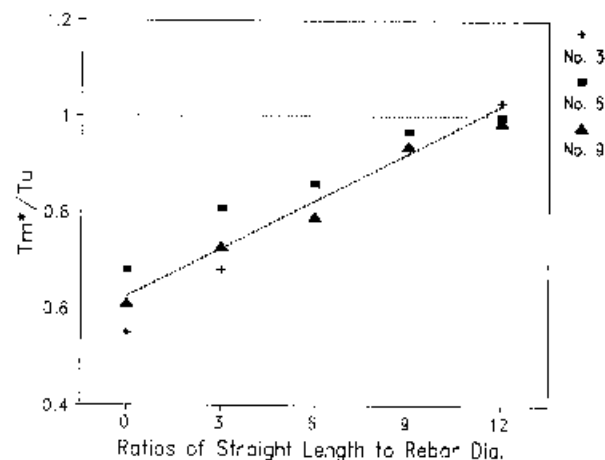


Fig. 19—Effect of straight embedment length on ratio of tensile force to ultimate tensile capacity of reinforcing bars

through all data points in Fig. 19. As shown, a straight embedment length of 11.3 times the bar diameter is adequate to provide a ratio of 1.0.

ACI 318-89 defines the development length of a hook as the distance measured from the critical section to the back face of the hook. This distance is equal to the sum of the straight embedment length, plus three bar diameters for the hook radius and an additional bar diameter for the tail portion of the reinforcing bar. Therefore, based on the data presented, it is concluded that the development length of 90-deg GFRP hooks can be taken as  $11.3 + 3 + 1 = 15.3$  times the bar diameter. Conservatively, it is recommended that the embedment length be taken as 16 times the bar diameter.

Note that the preceding recommendation does not include any capacity-reduction factor. Furthermore, these recommendations are to be considered in light of the limitations of the tested specimens. Additional studies are required before comprehensive design guidelines can be developed.

#### CONCLUSIONS

Thirty-six 90-deg hooked GFRP reinforcing bar specimens were tested. The effects of concrete compressive strength, radius of bend, tail length, and straight embedment length on bond behavior were studied. From these tests, it is concluded that:

1. Higher concrete compressive strength results in little gain in the maximum tensile stress in the bars. For specimens with  $r/d_b = 3.0$ , however, an increase in the compressive strength resulted in higher initial stiffness and lower maximum slip at failure.
2. Strength and stiffness of the specimens with  $r/d_b = 0$  were very low and a minimum  $r/d_b$  of 3 for GFRP hooks is recommended.
3. Additional tail length beyond 12 times the bar diameter had no beneficial effect on the tensile stress, slip, and initial stiffness of the bar. Therefore, use of a minimum tail length of 12 bar diameters is recommended.
4. Increase in the straight embedment length of the bars increases tensile stress and initial stiffness, and reduces the slip.

5. It is recommended that a development length equal to 16 times the bar diameter be used for 90-deg GFRP hooks.

### ACKNOWLEDGMENTS

Partial support for this study through NSF Grant No. MSS-9257344 is gratefully acknowledged. However, the results and conclusions are those of the authors and do not necessarily reflect the views of the sponsor. The reinforcing bars used in this study were manufactured by IGI, Inc., Houston, Texas.

### NOTATION

- $d_b$  = reinforcing bar diameter, in.  
 $E_i$  = initial stiffness, kips/in.  
 $f_c'$  = concrete compressive strength for each specimen, psi  
 $f_{avg}$  = average of  $f_c'$  for all 4000- or 8000-psi (28- or 56-MPa) concrete, psi  
 $f_s^*$  = adjusted maximum tensile stress of reinforcing bars, ksi  
 $L$  = straight embedment length, in.  
 $L_{dh}$  = development length, in.  
 $L'$  = tail length, in.  
 $r$  = radius of bend, in.  
 $RA$  = reinforcing bar axial fracture  
 $RS$  = reinforcing bar shear fracture  
 $S_{slip,max}$  = ultimate slip at loaded end, in.  
 $T$  = applied tensile load, kips  
 $T_s^*$  = adjusted ultimate applied tensile load, kips  
 $T_u$  = ultimate tensile capacity of reinforcing bars, kips  
 $\delta_a$  = loaded-end slip after correction for elastic elongation of reinforcing bar, in.  
 $\delta_e$  = elastic elongation of reinforcing bar, in.  
 $\delta_{nt}$  = loaded-end slip measured during testing, in.

### REFERENCES

- ACI Committee 318, 1989. "Building Code Requirements for Reinforced Concrete (ACI 318-89)," American Concrete Institute, Detroit, pp. 181-211.
- ACI Committee 408, 1992. "State-of-the-Art Report on Bond under Cyclic Loads," American Concrete Institute, Detroit, pp. 3-7.
- Ehsani, M. R., 1993. "Glass-Fiber Reinforcing Bars." *Alternative Materials for the Reinforcement and Dressing of Concrete*, J. L. Clarke, ed., Blackie Academic & Professional, London.
- Ehsani, M. R.; Saadatmanesh, H.; and Tao, S., 1993. "Bond of GFRP Rebars to Ordinary Strength Concrete," *ACI International Symposium on Non-Metallic Continuous Reinforcement*, Vancouver, British Columbia, Canada.
- Faza, S. S., and GangaRao, H. V. S., 1990. "Bending and Bond Behavior of Concrete Beams Reinforced with Plastic Rebars," *Transportation Research Record* 1290, pp. 185-193.
- Ferguson, P. M., and Thompson, J. N., 1962. "Development Length of High-Strength Reinforcing Bars in Bond," *ACI JOURNAL, Proceedings* V. 59, No. 7, pp. 887-921.
- Keesler, R. J., and Powers, R. G., 1988. "Corrosion of Epoxy-Coated Rebars—Keys Segmental Bridge—Monroe County," Report No. 88-8A, Florida Department of Transportation, Materials Office, Corrosion Research Laboratory, Gainesville.
- Larralde, J., and Silva, R., 1993. "Bond and Slip of FRP Rebars in Concrete," *Journal of Materials in Civil Engineering*, ASCE, V. 5, No. 1, pp. 30-40.
- Minor, J., and Jirsa, J. O., 1975. "Behavior of Bent Bar Anchorage," *ACI JOURNAL, Proceedings* V. 72, No. 4, pp. 141-149.
- Saadatmanesh, H., and Ehsani, M. R., 1991. "Fiber Composite Bar for Reinforced Concrete Construction," *Journal of Composite Materials*, pp. 188-203.
- Tao, S., 1994. "Bond of Glass Fiber Reinforced Plastic Rebars to Concrete," PhD dissertation, Department of Civil Engineering and Engineering Mechanics, University of Arizona, Tucson.
- Wu, W. P.; GangaRao H.; and Prucz, J. C., 1991. "Mechanical Properties of Fiber Reinforced Plastics," *Research Report*, Constructed Facilities Center, College of Engineering, West Virginia University.